

FIRST GLOBAL LINEAR GYROKINETIC SIMULATIONS IN 3D MAGNETIC CONFIGURATIONS

G. Jost, T.M. Tran, L.Villard, W.A. Cooper, K. Appert
*Centre de Recherches en Physique des Plasmas
 Association Euratom - Confédération Suisse
 Ecole Polytechnique Fédérale de Lausanne*

Introduction : In the recent past, the neoclassical theory has been the main focus of transport studies in alternative magnetic confinement devices. Today it is quite well developed and has served to identify configurations with enhanced neoclassical transport properties. On the other hand, the effects of microinstabilities on transport, though extensively investigated in tokamaks, have received little attention in 3D configurations. In a previous work [1], we presented a code aimed at the investigation of Ion Temperature Gradient (ITG) modes for such 3D magnetic configurations. This code has been successfully validated in axisymmetric configurations, but the computational time required by this version becomes prohibitive for full 3D cases. The code we present here is a modified version of this 3D code improved by the implementation of the extraction of the fast spatial variation [2]. The code meanwhile ported on a CRAY T3E is benchmarked against the helical version of the GYGLES code [3]. Results in a 3D configuration, namely a tokamak with a helical boundary deformation, are also presented.

Model and Implementation : The plasma is modeled by gyrokinetic ions and adiabatic electrons, and the code follows the time evolution of quasi-neutral electrostatic perturbations of the local Maxwellian distribution function f_0 [1]. The MHD equilibrium code VMEC provides the magnetic configurations [4]. We write the electrostatic potential as

$$\phi(s, \theta^*, \varphi, t) = \text{Re} \left(\tilde{\phi}(s, \theta^*, \varphi, t) e^{iS(s, \theta^*, \varphi)} \right), \quad S(s, \theta^*, \varphi) = m_0 \theta^* + n_0 \varphi$$

where (s, θ^*, φ) are the PEST-1 coordinates, $s = \Phi/\Phi_0$ where $2\pi\Phi$ is the toroidal flux, θ^* a poloidal angle which makes the field lines straight, φ is the geometric toroidal angle, $\tilde{\phi}$ is the extracted potential, S is the fast spatial phase, m_0 and n_0 are integer numbers which are both input parameters of the code. The ITG driven modes being aligned with the magnetic lines, i.e. $k_{\parallel} \ll k_{\perp}$, we choose $m_0 \approx n_0 q(s_0)$, with $q(s_0)$ the safety factor at $s = s_0$ where the ion temperature gradient peaks.

Using the same transformation for the perturbed ion distribution function f , the code now solves the following system of equations :

$$\frac{d\vec{R}}{dt} = v_{\parallel} \vec{h} + \frac{v_{\parallel}^2 + v_{\perp}^2/2}{\Omega} \vec{h} \times \frac{\vec{\nabla} B}{B}, \quad \frac{dv_{\parallel}}{dt} = \frac{1}{2} v_{\perp}^2 \vec{\nabla} \cdot \vec{h}, \quad \frac{d\mu}{dt} = 0,$$

$$\frac{en_0}{T_e} \tilde{\phi}(\vec{x}) - (i\nabla_{\perp} S + \nabla_{\perp}) \cdot \left[\frac{n_0}{B\Omega} (i\nabla_{\perp} S + \nabla_{\perp}) \tilde{\phi}(\vec{x}) \right] = \tilde{n}_i(\vec{x}),$$

$$\tilde{n}_i(\vec{x}) = \int \tilde{f}(\vec{R}, v_{\parallel}, v_{\perp}) \delta^3(\vec{R} - \vec{x} + \vec{\rho}) e^{i(S(\vec{R}) - S(\vec{x}))} B d\vec{R} dv_{\parallel} d\mu,$$

$$\frac{d}{dt} \tilde{f} + i \frac{dS}{dt} \tilde{f} = - \frac{\langle \vec{E} \rangle \times \vec{B}}{B^2} \frac{\partial f_0}{\partial \vec{R}} - \frac{q_i}{m_i} \vec{h} \cdot \langle \vec{E} \rangle \frac{\partial f_0}{\partial v_{\parallel}} - \left(v_{\parallel} \frac{\partial f_0}{\partial v_{\parallel}} + \frac{1}{2} v_{\perp} \frac{\partial f_0}{\partial v_{\perp}} \right) \langle \vec{E} \rangle \cdot \vec{h} \times \frac{\vec{\nabla} B}{B^2},$$

$$\langle \vec{E} \rangle = -\frac{1}{2\pi} \int (i\nabla S + \nabla) \tilde{\phi}(\vec{x}) e^{-i(S(\vec{R}) - S(\vec{x}))} dx d\alpha,$$

where the symbols have their usual meaning [1].

The equations governing the ions have been discretized using a Particle-In-Cell scheme, and the gyrokinetic Poisson equation is solved in the PEST-1 magnetic system of coordinates using a finite element approximation for the extracted electrostatic potential $\tilde{\phi}$. We choose quadratic splines as finite element basis [1]. The RHS of the discretized Poisson equation is Fourier filtered in the poloidal and toroidal directions, we keep only some modes around (m_0, n_0) , the shape and the width of the filter being a function of the magnetic configuration.

As we now solve only the slow spatial variation of the potential, the number of grid points is independent of the toroidal wave number n , usually equal to the number of processors.

Results : We have compared the results obtained with the full 3D code and the helical version of the GYGLES code [3]. The helical GYGLES code is a 2D code aimed at the investigation of ITG modes in helically symmetric configurations. It solves the same system of equations, but in a helical system of coordinates (x', y') , with $x' = r \cos(\zeta)$, $y' = r \sin(\zeta)$, $\zeta = \theta - hz$, where (r, θ, z) are the cylindrical coordinates, and h the helicity. In GYGLES, Poisson's equation is solved in the (s_h, θ_h) magnetic coordinates, s_h is a normalized radial variable $\propto \psi_h^{1/2}$, where ψ_h is the helical flux, and θ_h is equal to $\tan^{-1}(y'/(x' - x'_M))$, $(x'_M, 0)$ is the position of the magnetic axis. The helical code uses an analytical vacuum solution [3] for the magnetic configuration.

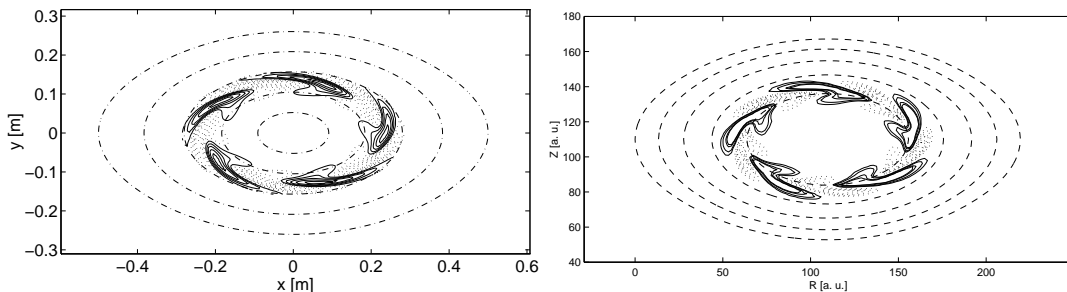


Figure 1: Level surfaces of the electrostatic potential ϕ in a straight $L=2$ configuration obtained with the helical GYGLES code in the (x', y') plane (left) and the full 3D code in the (R, Z) plane at $\varphi = 0$ (right). Dashed lines are the magnetic surfaces at $s_h = .2, .4, .6, .8, 1$ (left) and $s = .2, .4, .6, .8, 1$ (right). The ion temperature gradient peaks at $s_{h0} = 0.5 \equiv s_0 = 0.2$.

For this benchmark, we used the following procedure : for a given helical configuration, we obtained the position of the last magnetic surface ($s_h = 1$), from which we computed the Fourier coefficients $R_{m,n}(s = 1)$, $Z_{m,n}(s = 1)$ required by VMEC as input parameters [4] for the MHD equilibrium. We recomputed the configuration, and provided VMEC's results to the 3D code. Thus we tested also the interface between VMEC and the 3D code for a full 3D problem.

Comparisons were performed with two cases, a straight $L=2$ stellarator and a straight heliac configuration with a helicity $h = 1 m^{-1}$ and $B = 1 T$ at the magnetic axis. The equilibria computed by VMEC were centered at $R_{00} = 100 m$ with a number of field periods N_{per} equal to R_{00} , simulations were performed over one period. In the helical

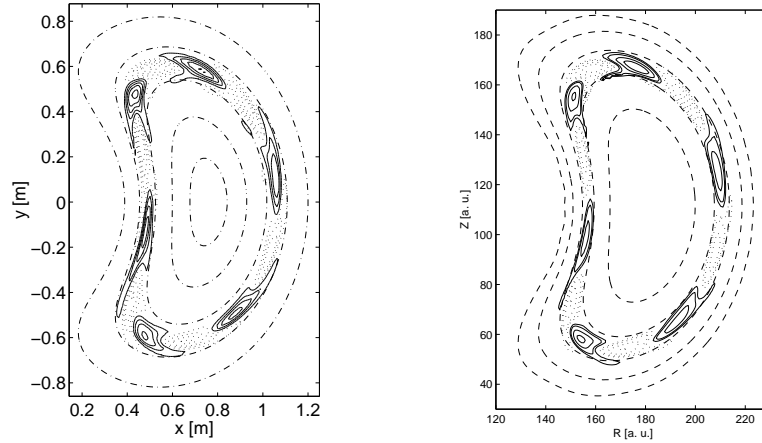


Figure 2: *Electrostatic potential ϕ in a straight heliac obtained with GYGLES in the (x', y') plane (left) and the full 3D code in the (R, Z) plane at $\varphi = 0$ (right). The ion temperature gradient peaks at $s_{h0} = 0.7 \equiv s_0 = 0.5$.*

system of coordinates, an ITG mode can be defined by a “helical” mode number n_h [3]. With a helicity $h = 1 m^{-1}$, we can easily show using the definitions of (x', y') than the toroidal mode number n is related to n_h by : $n/N_{per} = m - n_h$, where m is the poloidal mode number.

For the L=2 case (figure 1), the ion temperature gradient peaks at $s_{h0} = 0.5 \equiv s_0 = 0.2$, $a/L_T = 10$, $T_i(s_0) = 1keV$, $q(s_0) = 5.5$, and the density profile is flat. For a helical wave number $n_h = 4$, GYGLES produces a mode with a dominant poloidal mode number $m = 5$ and a frequency and a growth rate equal to 139.5 kHz and 52 kHz, respectively. With $m_0 = 5$ and $n_0/N_{per} = 1$, the frequency and the growth rate obtained with the 3D code agree well, being equal to 139 kHz and 55 kHz, respectively. The global shape of the mode agrees also for both codes, but the GYGLES code which solves the equations on a small portion of the s_h -axis, here between $s_h = 0.3$ and $s_h = 0.7$, provides a more precise picture of the mode than the 3D code which solves the problem in the whole radial domain $0 \leq s \leq 1$.

Figure 2 shows the comparison for the heliac case, here $n_h = 4.2$, the ion temperature gradient peaks at $s_{h0} = 0.7 \equiv s_0 = 0.5$, $a/L_T = 10$, $T_i(s_0) = 4keV$, $T_e/T_i(s_0) = 0.1 + 0.9(1 - s_h^2)$, the density profiles are flat. We choose $m_0 = 6$ and $n_0/N_{per} = 1.8$ and we keep the following modes by filtering : $(m_0 + i, n_0/N_{per} + i)$, $i = [-4, 4]$. Both codes produce a mode with a $m = 6$ dominant poloidal spectrum. The frequencies and growth rates 138 kHz and 40 kHz with GYGLES and 132 kHz and 34 kHz with the 3D code agree well.

The 3D simulations were performed with 4×10^6 particles, with 64 points in each direction (s, θ^*, φ) , they required ≈ 180 cpu-seconds per step with 64 processors on a CRAY T3E.

A first result with a 3D configuration is shown in figure 3. We choose a tokamak with an L=2 helical boundary deformation. The positions R, Z of the last magnetic surface $s = 1$ for the computation of VMEC equilibria are given by :

$$\begin{cases} R &= R_{00} + \cos(\theta) + \delta(\cos(\theta) + \cos(\theta - 2N_{per}\varphi)) \\ Z &= \sin(\theta) + \delta(\sin(\theta) - \sin(\theta - 2N_{per}\varphi)) \end{cases}$$

where θ is the geometric poloidal angle, δ is the amplitude of the boundary deformation,

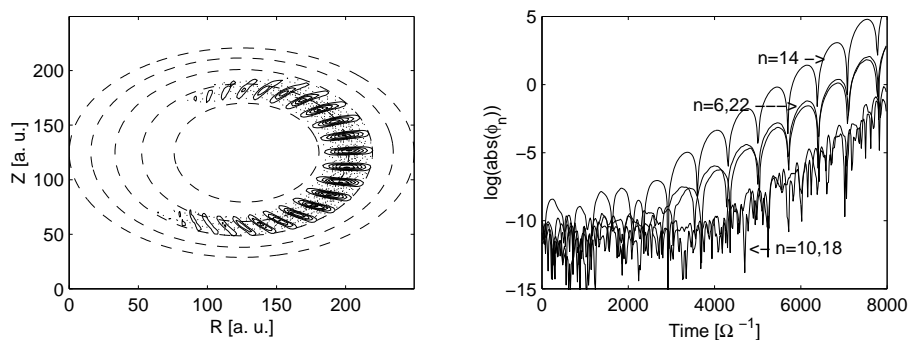


Figure 3: Level surfaces of the electrostatic potential ϕ in (R, Z) at $\varphi = 0$ and $t = 6000 \Omega^{-1}$ (left) and time evolution of the absolute value of the toroidal spectrum of the potential measured in $s = s_0$ and $\theta^* = 0$ (right), we show here only the modes $n = 6, 10, 14, 18, 22$.

$R_{00} = 4m$, $N_{per} = 4$, and the helicity of the perturbation is equal to $1 m^{-1}$. The safety factor is a parabolic function of the poloidal flux, the ion temperature gradient peaks at $s_0 = 0.4$ where $q(s_0) = 2.5$, $a/L_T = 3.6$, and $a/\rho = 96$ with ρ the Larmor radius at s_0 . In the tokamak case ($\delta = 0$), with these parameters, the maximum growth rate is obtained with $n = 14$ and is equal to $0.00208\Omega^{-1}$ with a frequency = $0.0054\Omega^{-1}$. Figure 3 shows the result for a perturbation $\delta = 0.15$, where we keep the following modes by filtering : $(m_i, n_j) = (m_0 + i + j, n_0/N_{per} + j)$, $i = [-6, 6]$, $j = [-8, 8]$ with $(m_0, n_0) = (34, 14)$. The ITG mode is now a 3D mode characterized by several toroidal modes numbers, its spectrum is centered around the mode $(34, 14)$. Figure 3 shows also clearly the effects of such L=2 deformation where only toroidal components satisfying $\text{mod}(n - n_0, 2N_{per}) = 0$ can couple with the component n_0 . However the growth rate and frequency of the 3D mode, which are equal to $0.0022\Omega^{-1}$ and $0.005\Omega^{-1}$ are not significantly modified by the helical deformation.

We applied also a L=3 helical boundary deformation to a tokamak, keeping the same equilibrium parameters. We again find that the growth rate and frequency are only slightly modified in comparison with the tokamak case.

Conclusion : The complete 3D model has been successfully validated in straight helical geometry and has permitted the first simulations of unstable global ITG modes in non-axisymmetric toroidal configurations. In these results, the effect of the helical deformation of the boundary on the growth rate and the frequency has, however, turned out to be weak. Further work will investigate the properties of other 3D geometries, particularly in quasi-symmetric configurations.

This work was partly supported by the Swiss National Science Foundation. The computations have been performed on the CRAY T3E of the Joint Computing Center of the Max Planck Gesellschaft and the IPP in Garching.

References

- [1] G. Jost *et al*, in Theory of Fusion Plasmas, Proc. Int. Workshop Varenna, (1998).
- [2] M. Fivaz *et al*, Comp. Phys. Comm. **111** (1998) 27.
- [3] L. Villard *et al*, in Theory of Fusion Plasmas, Proc. Int. Workshop Varenna, (1998).
- [4] S. P. Hirshman and D. K. Lee, Comp. Phys. Comm. **39** (1986) 161.